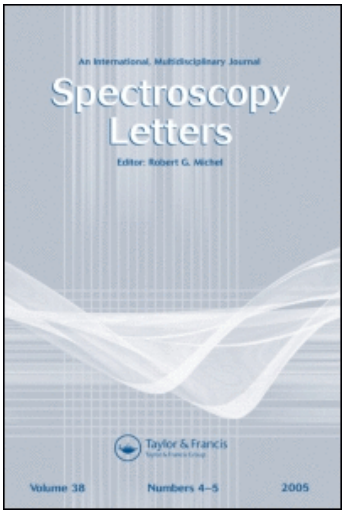

Spectroscopy Letters
Publication details, including instructions for authors and subscription information:
http://www.informaworld.com/smpp/title~content=t713597299

Solid-State ^{1}H-NMR Relaxation Properties of the Fruit of a Wild Relative of Eggplant at Different Proton Larmor Frequencies

Pellegrino Conte[a]; Salvatore Bubici[b]; Eristanna Palazzolo[a]; Giuseppe Alonzo[a]
[a] Dipartimento di Ingegneria e Tecnologie Agro-Forestali (DITAF), Università degli Studi di Palermo, Palermo, Italy [b] INVENTO s.r.l., Torino, Italy

To cite this Article Conte, Pellegrino , Bubici, Salvatore , Palazzolo, Eristanna and Alonzo, Giuseppe(2009) 'Solid-State ^{1}H-NMR Relaxation Properties of the Fruit of a Wild Relative of Eggplant at Different Proton Larmor Frequencies', Spectroscopy Letters, 42: 5, 235 — 239
To link to this Article: DOI: 10.1080/00387010902895038
URL: http://dx.doi.org/10.1080/00387010902895038

Spectroscopy Letters, 42:235–239, 2009

ISSN: 0038-7010 print/1532-2289 online
DOI: 10.1080/00387010902895038

Taylor & Francis
Taylor & Francis Group

Solid-State ^{1}H-NMR Relaxation Properties of the Fruit of a Wild Relative of Eggplant at Different Proton Larmor Frequencies

Pellegrino Conte[1], Salvatore Bubici[2], Eristanna Palazzolo[1], and Giuseppe Alonzo[1]

[1]Dipartimento di Ingegneria e Tecnologie Agro-Forestali (DITAF), Università degli Studi di Palermo, Palermo, Italy
[2]INVENTO s.r.l., Torino, Italy

ABSTRACT ^{1}H longitudinal relaxation time profiles (T1) at different proton Larmor frequencies were registered for a solid-state plant tissue by using fast field cycling (FFC) nuclear magnetic resonance (NMR) spectroscopy. T1 distributions were obtained and the curves deconvoluted in order to differentiate among the different T1 components. Among the components, two were assigned to hydrophobic (e.g., fatty acid) and hydrophilic (e.g., saccharide) molecular systems, whereas the others were attributed to bulk and bound water. This paper shows for the first time solid-state FFC-NMR spectroscopy applied to plant tissue and reveals that relaxometry is a very promising technique for studying plant systems.

KEYWORDS eggplant, FFC-NMR relaxometry, molecular dynamics, NMRD profile, nuclear magnetic resonance spectroscopy, plant systems

INTRODUCTION

Nuclear magnetic resonance (NMR) relaxation studies at low magnetic fields probe the molecular dynamics of very complex systems such as food,[1–5] seeds,[6,7] archaeological materials,[8] nanoporous media,[9] and environmental matrices[10] through measurements of longitudinal (T1) and transversal (T2) relaxation times.[11–14]

In the basic NMR dispersion (NMRD) or fast field cycling NMR (FFC-NMR) setup, the Zeeman magnetic field (B_0) cycles through three different values usually indicated as B_{pol}, B_{relax}, and B_{acq}.[12,13] B_{pol} is applied for a limited and fixed period of time in order to achieve magnetization saturation and sensitivity enhancement.[12] Then, the magnetic field is switched to a new one, B_{relax}, applied for a period (τ) during which the intensity of the magnetization changes (or relaxes) to reach a new equilibrium condition. Finally, the application of the magnetic field B_{acq} makes the magnetization observable and the free induction decay (FID) acquirable. The relaxation times of the observed nuclei are obtained at each fixed B_{relax} intensity through a progressive variation of the τ values. The set of relaxation times measured by changing the intensity of B_{relax} describes the variations of the longitudinal relaxation rates ($R1 = 1/T1$) as a function of the applied

Received 11 July 2008;
accepted 19 January 2009.

Address correspondence to Pellegrino Conte, Dipartimento di Ingegneria e Tecnologie Agro-Forestali (DITAF), Università degli Studi di Palermo, v.le delle Scienze 13, ed. 4, 90128 Palermo, Italy. E-mail: pellegrino.conte@unipa.it

magnetic field strength.[14] The R1 versus B_{relax} curves represent the NMRD profiles. Such profiles can be related to physical/chemical properties of complex materials.[11–14] For example, ^{1}H-NMRD analyses of hen eggs revealed that quality loss during the first few days of storage can be associated with acidity increase arising from carbon dioxide diffusion through the eggshell,[15] while two-stage gelation process (first formation of strongly linked dimers, then weak interdimer aggregations) was discovered for $CaCl_2$ low methoxyl pectin water solutions.[16] Moreover, NMRD investigations were also used to study the binding sites of some globular proteins[17] and the catalytic properties of metalloporphyrins.[18]

Up to now, the majority of the NMRD measurements were done in the liquid or semisolid state.[11] Only few works have been done in the solid state. This is due to technical limits related to the general rapid relaxation times of solid systems, which demand high-power pulses and fast receiver and probe recovery after excitation for characterization.[11]

In this paper, preliminary results on ^{1}H-NMRD analyses of the fruit of a wild relative of eggplant are described. Solid-state longitudinal relaxation time (T1) profiles are discussed, and the different T1 components are assigned to the various molecular systems forming the fruit tissues of the wild relative of eggplant.

MATERIALS AND METHODS

Sample

Fruit samples from *Solanum aethiopicum* gr. *integrifolium* (a wild relative of *Solanum melongena* L.) were obtained from the Consiglio per la Sperimentazione in Agricoltura–CRA (Montanaro Lombardo, Italy). Ten fruits of the wild relative of eggplant were first freeze-dried, then powdered by using liquid N_2 and mixed to obtain a homogeneous mixture. The solid mixture was analyzed without further manipulation.

NMRD Experiments and Data Elaboration

^{1}H-NMRD data were recorded on a Stelar Spinmaster-FFC-2000 field-cycling relaxometer (Stelar S.n.c., Mede, PV, Italy) at a temperature of 300 K and by measuring the longitudinal magnetization evolution at different magnetic field strengths (B_{relax}, see the Introduction for other details) corresponding with proton Larmor frequencies of 0.01, 0.1, 1, 10, and 20 MHz. Proton spins were first polarized at B_{pol} see the Introduction for 0.1 s. The magnetic field was then switched to B_{relax}, (see the Introduction) which was applied for a period τ arrayed with 64 values varying from 1 to 1000 ms. τ array was chosen in a geometric progression in order to cover the entire relaxation curve of interest. Finally, a 16.3-MHz B_{acq} was used to obtain observable magnetization and reveal free induction decay (FID) with a time domain of 512 points. Eight scans were accumulated. The experimental data were processed with the UPEN algorithm (Alma Mater Studiorum–Università di Bologna), thereby obtaining T_1 distributions.[19,20] The T_1 distribution curves were exported to OriginPro 7.5 SR6 (version 7.5885; OriginLab Corporation, Northampton, MA, USA) in order to perform deconvolution with Gaussian functions and to recover the different components giving rise to the longitudinal relaxation time distributions. The Gaussian curves were combined to obtain the best fitting of the experimental data. Deconvolution was considered optimum when the coefficient of determination (R^2) for the best fitting resulted $\geq$0.98.

RESULTS AND DISCUSSION

Figure 1 shows the T1 distributions of the wild relative of the eggplant fruit at different proton Larmor frequencies (^{1}H LF). All the distributions were deconvoluted (dotted curves) to recover information on the different T1 components provided by the experimental data (black dots). The full lines in Figure 1 were obtained as combination of the deconvoluted dotted curves in order to retrieve the best fitting of the experimental data (see Materials and Methods).

With the exception of the T1 distribution at the ^{1}H LF = 1 MHz (Fig. 1c), a component at T1 = 100 ms was observed when ^{1}H LF was 0.01, 0.1, 10, and 20 MHz (Figs. 1a, b, d, and e, respectively). A second component appeared at 30 ms in the distributions at 0.01, 0.1, and 10 MHz (Figs. 1a, b, and d, respectively), whereas the profile at ^{1}H LF = 20 MHz revealed a component at T1 = 50 ms (Fig. 1e).

According to Jóhannesson et al.,[17] dispersionless T1 NMRD profiles (i.e., no T1 changes with 1H

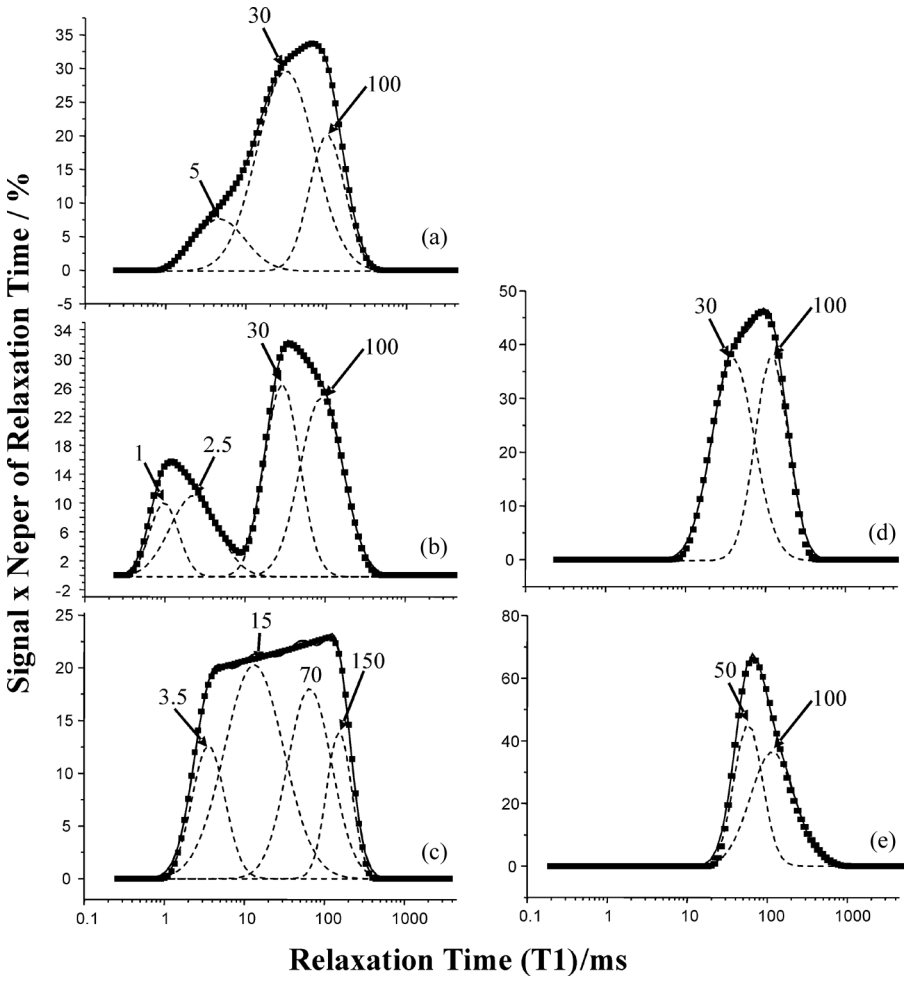

FIGURE 1 T1 profiles of the eggplant fruit at different proton Larmor frequencies (^{1}H LF). (a) ^{1}H LF = 0.01 MHz; (b) ^{1}H LF = 0.1 MHz; (c) ^{1}H LF = 1 MHz; (d) ^{1}H LF = 10 MHz; (e) ^{1}H LF = 20 MHz. The black dots are the experimental data. The dashed lines represent the different T1 components as obtained by deconvolution. The full lines are the fitting of the experimental data obtained by deconvolution.

Larmor frequency) can be associated with non–water-interacting molecular systems. Conversely, T1 dispersion (i.e., changes of T1 value with the proton Larmor frequency) is observed when water interacts with hydrophilic organic materials.

Plant systems are very complex systems where hydrophilic moieties (e.g., polysaccharides in cell membrane structures) are localized near hydrophobic structures such as, for example, those building the phospholipid bilayers in cell membranes. Moreover, many other molecules are inside cell membranes. Among those, cell-water–dissolved secondary metabolites must also be considered.[21]

Due to molecular complexity, it was impossible to univocally assign to a sole specific molecule both T1 dispersiveless and T1 dispersive components. However, it can be reasonably hypothesized that the dispersiveless component at 100 ms was due to the molecular hydrophobic systems, which are distant from cell water.[17] On the contrary, the T1 dispersive component can be assigned to the hydrophilic cell moieties,[17] such as polysaccharides, which may directly interact with the cell water still present in the fruit sample of the wild relative of the eggplant.

Figures 1a and 1b also show a broad T1 distribution in the shortest T1 interval. This T1 distribution contains only one component centered at 5 ms at ^{1}H LF = 0.01 MHz (Fig. 1a), whereas it reveals two components (centered at 1 and 2.5 ms, respectively) at ^{1}H LF = 0.1 MHz (Fig. 1b). Clearly, the broad T1 distribution in the shortest T1 interval is made by T1 dispersive components.

Having already assigned hydrophobic and hydrophilic moieties to the distribution at the longest longitudinal proton relaxation times, the only other

proton-rich molecular system to be considered is the intracell water still present in the freeze-dried plant fruit cells.

As reported in the literature,[22] two different kinds of water must be distinguished in complex H_2O-containing systems: a slow-moving bound water and a fast-moving bulk water. Because longitudinal proton relaxation time values in the solid-state NMR are directly related to molecular motions (the faster the molecular motions, the shorter are the T1 values),[23] it can be argued that the T1 value for the bound water must be longer than that of the bulk H_2O. According to this interpretation, the component at 2.5 ms can be assigned to bound water, whereas that at 1 ms must be attributed to bulk water.

The T1 distributions of both H_2O components collapsed together at ^{1}H LF = 0.01 MHz (Fig. 1a). At the moment, due to a lack of literature on this subject, no explanations are available to understand why the two water components were undistinguishable at the lowest ^{1}H LF value. Deeper NMRD investigations are needed to comprehend the T1 behavior at the lowest B_{relax} values of water systems in plant tissues.

In the current paper, the T1 profile recovered at the proton Larmor frequency of 1 MHz is not discussed. Figure 1c shows that the T1 distribution at ^{1}H LF = 1 MHz presents a very broad plateau. To the best of our knowledge, there are no explanations available in literature to understand why the plant tissue sample used in this study behaved as reported in Figure 1c. It must be stated that the deconvolution pattern reported in Figure 1c is only an attempt to find the best fitting for the experimental results. Many other deconvolution patterns, equally satisfying from a mathematical point of view, were found to fit as well for the experimental data. All the deconvolution patterns were made by T1 components appearing in several different positions, thereby preventing any definitive conclusion on the nature of the components giving rise to the profile at 1 MHz (Fig. 1c).

CONCLUSIONS

To the best of our knowledge, this preliminary study reported for the first time solid-state NMRD profiles of plant tissues. Namely, analyses of the fruit from *Solanum aethiopicum* gr. *integrifolium*, which is a wild relative of *Solanum melongena* L., were carried out. Two different T1 components assigned to hydrophobic (e.g., fatty acid) and hydrophilic (e.g., polysaccharide) organic systems were recognized. Moreover, two other T1 components were assigned to the bulk and the bound water normally present in plant tissues. However, due to the preliminary nature of this work, further studies on solid-state NMRD profiles of plant tissues are needed for a better comprehension of the dependency of the T1 components on the proton Larmor frequency values. Notwithstanding the limits of the technique (it is a low-field NMR approach, thereby preventing the recovering of classic high resolved NMR fingerprintings), this preliminary study, done on freeze-dried plant tissues, suggests that NMRD spectroscopy holds a great potential also for the characterization of intact and still living plant systems.

ACKNOWLEDGMENTS

The authors are grateful to Dr. G.L. Rotino (Consiglio per la Sperimentazione in Agricoltura–CRA, Montanaro Lombardo, Italy) for having provided the eggplant fruit samples. Dr. G. Ferrante (Stelar s.r.l., Mede, Italy) is kindly acknowledged for the NMRD facilities. Dr. V. Bortolotti (Università di Bologna, Italy) is acknowledged for his assistance in the use of UPEN software.

REFERENCES

1. Davenel, A.; Schuck, P.; Mariette, F.; Brulé, G. NMR relaxometry as a non-invasive tool to characterize milk powders. *Lait* **2002**, *82*, 465–473.
2. Bertram, H. C.; Wiking, L.; Nielsen, J. H.; Andersen, H. J. Direct measurement of phase transitions in milk fat during cooling of cream–a low field NMR approach. *Int. Dairy J.* **2005**, *15*, 1056–1063.
3. Hernández-Sánchez, N.; Hills, B. P.; Barreiro, P.; Marigheto, N. An NMR study on internal browning in pears. *Postharvest Biol. Technol.* **2007**, *44*, 260–270.
4. Gianferri, R.; Maioli, M.; Delfini, M.; Brusio, E. A low-resolution and high-resolution nuclear magnetic resonance integrated approach to investigate the physical structure and metabolic profile of mozzarella di bufala Campana cheese. *Int. Dairy J.* **2007**, *17*, 167–176.
5. Tang, H. R.; Zhao, B.- L.; Belton, P. S.; Sutcliffe, L. H.; Ng, A. Anomalous proton NMR relaxation behaviour of cell wall materials from Chinese water chestnuts. *Magn. Res. Chem.* **2000**, *38*, 765–770.
6. Colnago, L. A.; Eugelsberg, M.; Souza, A. A.; Barbosa, L. L. High-throughput non destructive determination of oil content in intact seeds by continuous wave-free precession NMR. *Anal. Chem.* **2007**, *78*, 1271–1274.
7. Prestes, R. A.; Colnago, L. A.; Forato, L. A.; Vizzotto, L.; Novotny, E. H.; Carrilho, E. A rapid and automated low resolution NMR method to analyze oil quantity in intact oilseeds. *Anal. Chim. Acta* **2007**, *596*, 325–329.

8. Casieri, C.; Bubici, S.; Viola, I.; De Luca, F. A low-resolution non invasive NMR characterization of ancient paper. *Solid State Nucl. Magn. Reson.* **2004**, *26*, 65–73.
9. Kausik, R.; Fatkullin, N.; Hüsing, N.; Kimmich, R. Investigations of polymer dynamics in nanoporous media by field cycling NMR relaxometry and the dipolar correlation effect. *Magn. Reson. Imaging* **2007**, *25*, 489–497.
10. Melton, J. R.; Kantzas, A.; Langford, C. H. Nuclear magnetic resonance relaxometry as a spectroscopic probe of the coordination sphere of a paramagnetic metal bound to a humic acid mixture. *Anal. Chim. Acta* **2007**, *605*, 46–52.
11. Wang, Y. L.; Belton, P. S. Application of fast field cycling proton NMR relaxation spectroscopy to a crystalline solid. *Chem. Phys. Lett.* **2000**, *325*, 33–38.
12. Kimmich, R.; Anoardo, E. Field-cycling NMR relaxometry. *Prog. Nucl. Magn. Reson. Spectrosc.* **2004**, *44*, 257–320.
13. Ferrante, G.; Sykora, S. Technical aspects of fast field cycling. *Adv. Inorg. Chem.* **2005**, *57*, 405–470.
14. Halle, B.; Johannesson, H.; Venu, K. Model-Free Analysis of stretched relaxation dispersions. *J. Magn. Res.* **1998**, *135*, 1–13.
15. Laghi, L.; Cremonini, M. A.; Placucci, G.; Sykora, S.; Wright, K.; Hills, B. A proton NMR relaxation study of hen egg quality. *Magn. Reson. Imaging* **2005**, *23*, 501–510.
16. Dobies, M.; Kuśmia, S.; Jurga, S. ^{1}H NMR and rheological studies of the calcium induced gelation process in aqueous low methoxyl pectin solutions. *Acta Phys. Pol. A.* **2005**, *108*, 33–46.
17. Jóhannesson, H.; Denisov, V. P.; Halle, B. Dimethyl sulfoxide binding to globular proteins: a nuclear magnetic relaxation dispersion study. *Protein Sci.* **1997**, *6*, 1756–1763.
18. Bryant, L. H.; Mercier, G. A. Relaxometric investigation of functional group placement on MnTPP derivatives supports the role of the molecular electrostatic potential maps as a tool to design new metalloporphyrins with larger relaxivities. *Int. J. Mol. Sci.* **2001**, *2*, 140–147.
19. Borgia, G. C.; Brown, R. J. S.; Fantazzini, P. Uniform-penalty inversion of multiexponential decay data. *J. Magn. Reson.* **1998**, *132*, 65–77.
20. Borgia, G. C.; Brown, R. J. S.; Fantazzini, P. Uniform-penalty inversion of multiexponential decay data II: data spacing, T2 data, systematic data errors, and diagnostics. *J. Magn. Reson.* **2000**, *147*, 273–285.
21. Taiz, L.; Zeiger, E. *Plant Physiology*, **4th ed.**; Sinauer Associates: Sunderland, MA, 2006.
22. Berti, F.; Costantino, P.; Fragai, M.; Luchinat, C. Water accessibility, aggregation, and molecular features of polysaccharide-protein conjugate vaccines. *Biophys. J.* **2004**, *86*, 3–9.
23. Conte, P.; Spaccini, R.; Piccolo, A. State of the art of CPMAS ^{13}C NMR spectroscopy applied to natural organic matter. *Prog. Nucl. Magn. Reson. Spectrosc.* **2004**, *44*, 215–223.